Outwards transport of angular momentum in a shallow water accretion disk experiment

F. Günzkofer [1,2] and P. Manz [3,2,1]

[1]*Physik-Department E28, Technische Universität München, James-Franck-Strasse 1, 85748 Garching, Germany*
[2]*Max-Planck-Institut für Plasmaphysik, Boltzmannstrasse 2, 85748 Garching, Germany*
[3]*Institute of Physics, University of Greifswald, 17489 Greifswald, Germany*

Accretion disks are a ubiquitous phenomenon in astrophysics. To be consistent with observations, there must be an as yet unknown mechanism for angular momentum redistribution. In laboratory experiments, especially, the two-dimensional geometry and the magnetohydrodynamic characteristics of an accretion disk are difficult to reproduce. Here we propose the design of a shallow water experiment in accretion disk geometry, where differential rotation is induced in a quasi-two-dimensional shallow water layer with an open surface that allows direct measurement of the radial and azimuthal fluid dynamics. The effect of the magnetic field is mimicked by established equivalence of magnetohydrodynamic and viscoelastic fluids. We demonstrate radial outwards transport of angular momentum in an accretion disk laboratory experiment. Therefore, the proposed experimental setup can help us to identify the origin of angular momentum redistribution in accretion disks.

I. INTRODUCTION

Accretion disks are one of the most common astrophysical phenomena. Since the disk particles rotate on stable Keplerian orbits (with an angular velocity $\Omega \propto r^{-3/2}$ and radius r), the gas cannot accrete directly onto the central object without first losing angular momentum. How angular momentum is transported outwards to spin up the outer parts of the accretions disk and decelerate the inner parts to spiral onto the central object is one of the central questions. As molecular viscosity in accretion disks is small, an anomalous viscosity is needed to transport the angular momentum outwards. Turbulence can provide such anomalous viscosity. A possible instability leading to outwards momentum transport is the magnetorotational instability (MRI) [1] driven by weak magnetic fields. Due to the high conductivity of the accretion disk plasma, magnetic field lines are frozen in and connect particles at different orbit radii similar to springs. The sheared rotation then leads to angular momentum transport from the inner to the outer particle [2].

There have been substantial efforts to demonstrate the MRI in laboratory experiments using different approaches to obtain sheared rotation of a magnetohydrodynamic (MHD) fluid. Experiments using a liquid gallium alloy were conducted in Taylor-Couette geometry and various magnetic field geometries [3–5]. Evidence for the magnetorotational instability in such experiments was found by investigating fluctuations of the coaxial fluid flow [4,5]. Other approaches included the use of liquid sodium in differential rotating spheres [6] and experiments with plasmas [7,8] in Taylor-Couette geometry. Though Ref. [6] reported signs of the MRI, it should be mentioned that numerical simulations suggested these are rather caused by different instabilities [9,10]. Therefore, any experimental findings on the MRI have to be carefully assessed in light of other possible
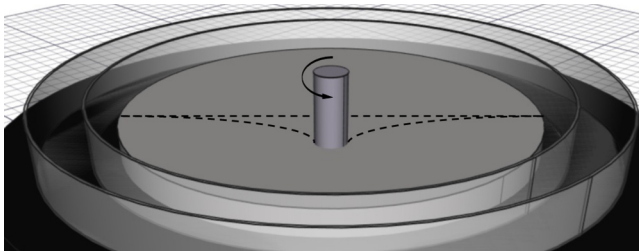
FIG. 1. Computer-aided design schematic of a reciprocal shaped fluid pool experiment to replicate an accretion disk geometry.

instabilities. To the best of our knowledge, enhanced outwards transport of angular momentum has not been demonstrated so far in any Taylor-Couette laboratory experiment.

We wonder if perhaps another geometry might be better suited to study the MRI. The experimental setup of the shallow water analog of the standing accretion shock instability [11] seems to represent the geometry of the accretion disk more naturally. The setup would additionally have the practical advantage of an open fluid surface allowing for measurements of radial-azimuthal fluid dynamics, which are necessary to estimate radial angular momentum transport. However, the shallow depth of the experiment is a concern since enhanced viscous damping is to be expected compared to the Taylor-Couette geometry. Furthermore, we were not sure whether angular momentum can be introduced into the system at all. We decided to give it a try.

This paper is organized as follows: In Sec. II the experimental setup is introduced. Angular rotation profiles are measured in water (Sec. III) and compared to a viscoelastic fluid mimicking MHD effects (Sec. IV).

II. EXPERIMENTAL SETUP

We propose an experiment with geometry similar to the one used to study the standing accretion shock instability [11]. A schematic depiction is shown in Fig. 1. Similar to Taylor-Couette geometry experiments, it exhibits inner and outer radii of $r_{in} = 26$ mm and $r_{out} = 250$ mm, respectively. However, the upper boundary is a free surface, and the lower boundary has a reciprocal shape,

$$H(r) = -\frac{1000\,\text{mm}^2}{r} + 4\,\text{mm}, \tag{1}$$

leading to a very small aspect ratio $H/(r_{out} - r_{in}) \ll 1$ resembling accretion disk geometry. In standing accretion shock experiments, this lower boundary profile mimics a gravitational potential due to the shallow water approximation [11,12]. Details on the experimental setup used here can be found in Ref. [12]. Different from the standing accretion shock instability experiment [12], the central cylinder is placed above the filling level, so no radial flow is forced externally. External momentum input is provided by rotation of the central drain. Rotation of the inner cylinder is obtained by attachment of a stepper motor, and angular momentum is thereby induced into the fluid. Due to the shallow water analogy, a constant height h above the ground profile [see Eq. (1)] favors Keplerian rotation. However, the pool is completely filled with fluid and thus in this experimental setup does not yield Keplerian rotation since the lower boundary does not affect the surface rotation. This setup resembles a Taylor-Couette-like experiment with a stationary outer cylinder. Compared to a flat bottom boundary, the reciprocal ground profile in Eq. (1) significantly enlarges the ratio of the drain to the bottom boundary and thereby allows for better momentum induction to the fluid at a low thickness to radius ratio of the fluid disk. Though not necessarily Keplerian, differential rotation is obtained nevertheless, and the quasi-two-dimensional geometry of an accretion disk is replicated. Additionally, the open surface allows *in situ* measurements of the radial and azimuthal
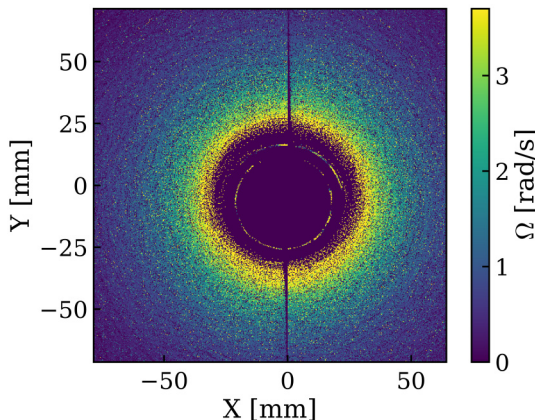
FIG. 2. Ω map of water rotating in the pool as obtained by means of particle tracking velocimetry.

flow and thereby direct detection of angular momentum transport. The height of the fluid h does not imitate the actual height of the accretion disk, which increases with the radius.

The MHD character of the accretion disk matter is central to the MRI mechanism. While both Reynolds and Maxwell stresses contribute to outwards transport of angular momentum, theoretical analysis has shown that this transport is dominated by the Maxwell stress for rotation profiles $\Omega(r)$ expected in accretion disks [13]. Plasma matter or liquid metals rotating in an external magnetic field are important for replication of an accretion disk system. However, such experiments require a rather expensive experimental setup. Magnetic field lines acting as elastic springs within an MHD fluid can be replicated using a viscoelastic solution of long-chain polymers in water [14,15]. The resulting polymeric stress tensor is similar to the magnetic stress tensor in MHD equations. Analytical and numerical investigations have shown the existence of an MRI-type instability for rotating viscoelastic fluids in Taylor-Couette geometry [15,16]. Experiments found an instability analog to the MRI by analyzing the coaxial mode numbers [17]. In the presented experimental prototype, experiments were carried out with a viscoelastic solution to mimic MHD effects due to cost constraints. For comparison, experiments using only water to switch off any effects from MHD/viscoelastics were performed.

The flow fields at the fluid surface are determined by particle tracking velocimetry based on the Crocker-Grier algorithm [18]. Small tracer particles (polypropylene spheres, $d = 3$ mm, $\rho = 0.9$ g cm^{-3}) are placed on the surface and move with the fluid flow. With a camera mounted approximately 1.4 m above the pool, the particle motion can be tracked. The particle velocities at different locations on the surface can be calculated, and thereby, the fluid rotation at different positions of the surface can be determined.

III. ROTATION PROFILES IN WATER

Whether hydrodynamic instabilities contribute to angular momentum transport in accretion disks by a non-negligible amount has not been finally determined yet [19]. Experimental evidence so far indicates the influence of hydrodynamic instabilities is small [20]. We first describe the experiments performed in water. Figure 2 shows the rotational frequency $\Omega(x, y)$ in water in the central parts of the pool.

The azimuthal symmetry of the rotation shown in Fig. 2 allows for the calculation of the rotation profile. By means of particle tracking velocimetry, a differential rotation profile $\Omega(r) \propto r^{-2.14}$ is found for water rotation in the region $26 < r < 120$ mm. The fitted exponent depends on the considered radial range and generally steepens if only outer regions are considered. However, $d \ln \Omega / d \ln r < -2$ holds for any choice of radial range. The capability of the particle tracking
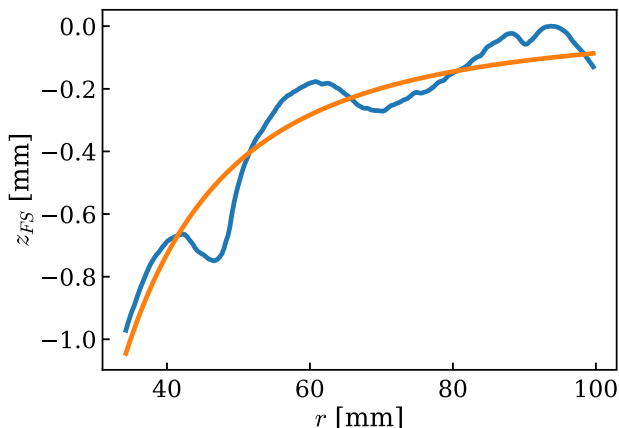
FIG. 3. Radial height profile (blue) shows that the measured $\Omega(r)$ results from an equilibrium of the surface height gradient which can be obtained from the fit function (orange) and centrifugal force.

velocimetry method can be tested by using the Fourier transform profilometry (FTP) established in previous experiments [12]. The FTP allows us to measure height shifts at the free water surface z_{FS}. For stationary rotation, equilibrium of the surface profile gradient and the centrifugal force due to rotation gives $dz_{FS}/dr = \Omega(r)^2 r$, which allows us to compare rotation and height measurements. Figure 3 shows the averaged surface height profile $z_{FS}(r) \propto r^{-2.33\pm0.06}$, which fits the expected $dz_{FS}/dr \propto r^{-3.28}$ quite well.

The radial decrease in angular frequency is much stronger than for the Keplerian case $\Omega(r) \propto r^{-3/2}$ in accretion disks. As mentioned above, the measured profile does not fulfill the requirements of a quasi-Keplerian profile since $|r^2\Omega|$ decreases with the radius as well. Such a rotation profile with $d\ln\Omega/d\ln r < -2$ is susceptible to Rayleigh's centrifugal instability. Presumably, the $\Omega \propto r^{-2.14}$ profile is the result of a balance between angular momentum transport by the Reynolds stress driven by the centrifugal instability and the bottom boundary drag damping the profile. Such a balance can lead to a stationary rotation profile.

Figure 4 shows the rotation profiles $\Omega(r)$ averaged over consecutive time intervals. It can be seen that $\Omega(r) \propto r^{-2.14}$ remains constant for water even over longer time spans up to at least 18 min.
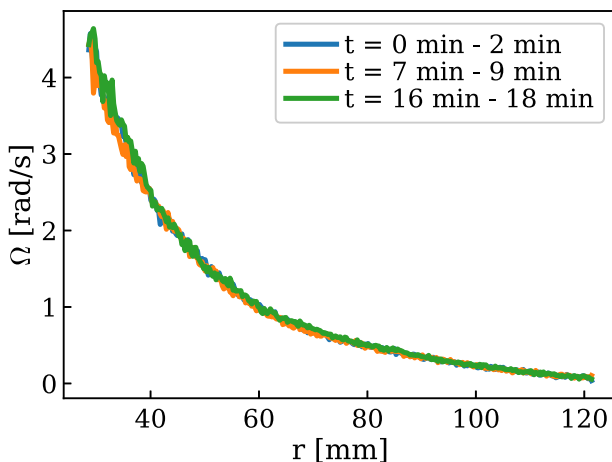

FIG. 4. Rotation profiles of purely hydrodynamic fluids are stable even for long rotation spans.
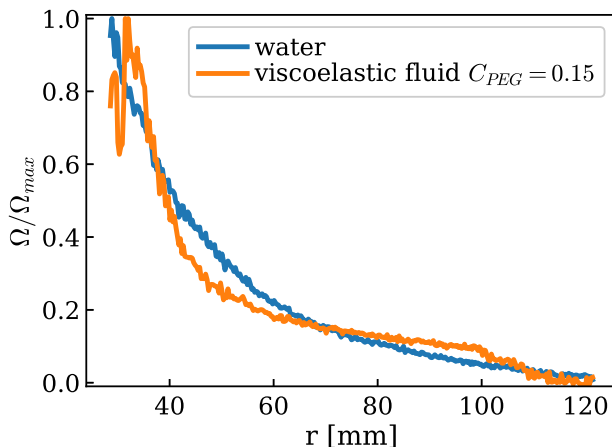
FIG. 5. Rotation profile comparison for water and a viscoelastic fluid (corresponding to $t = 120$–$240\,\mathrm{s}$ after the drain rotation started in Fig. 7). Due to the higher momentum transfer from the central cylinder to the viscoelastic fluid compared to water, the rotation profiles are given in relative terms.

The drain rotation starts at $t = 0$, and the data acquisition starts subsequently. Although it takes a few seconds for the water disk to spin up, this is not visible after averaging over a 2 min interval. However, the kinematic viscosity ν of water and the observed area $A = \pi \times (120\,\mathrm{mm})^2$ allow us to estimate the viscous momentum diffusion time $\tau = A/\nu \gg 18\,\mathrm{min}$. This estimate already indicates that viscous momentum diffusion is negligible compared to other momentum transport processes.

The ground friction dampens the rotation profile towards $\Omega \to 0$. Since the ground friction acts as a momentum sink especially in the shallower outer region of the pool, some process of outwards angular momentum transport is required to maintain a stationary rotation profile $\Omega(r)$. The steep gradient of the rotation profile $d \ln \Omega / d \ln r < -2$ explicitly allows Rayleigh's centrifugal instability, and therefore, the obtained results can be explained without other hydrodynamic instabilities which might play a role for accretion disk dynamics. This result is in good agreement with the results found in Ref. [20]. However, the presence of nonlinear instabilities, which are also discussed for accretion disks [19], in addition to the centrifugal instability cannot be ruled out. Such instabilities are generally not expected to occur at the Reynolds numbers expected in the experiments presented here, $\mathrm{Re} \lesssim 4000$ [20].

IV. ROTATION PROFILES IN A VISCOELASTIC FLUID

The same measurements were performed with the described viscoelastic polymer solution instead of water. The preparation of a viscoelastic fluid is based on the investigations done in Ref. [21]. A solution of polyethylene glycol (PEG) and polyethylene oxide (PEO) is used, where PEO—as a very-long-chain polymer—contributes the elastic properties of the fluid. For the measurements presented here, the concentrations are $C_{PEG} = 15\%$ and $C_{PEO} = 1000\,\mathrm{ppm}$.

Figure 5 shows a comparison of the rotation profiles for water and a viscoelastic fluid. Due to the process of rod climbing caused by the Weissenberg effect [22], flow measurements close to the inner cylinder are not possible in a reliable way. At radii larger than 100 mm, fluid rotation is dominated by the increased influence of ground friction. The rotation is damped towards $\Omega \to 0$. Therefore, the region of interest of the shown measurements is restricted to radii of $35 < r < 100\,\mathrm{mm}$.

The most prominent feature of the profile comparison is the region of profile flattening for $45 \lesssim r \lesssim 100\,\mathrm{mm}$, as expected for enhanced outwards transport of angular momentum. The accompanying region of profile steepening at $35 \lesssim r \lesssim 45\,\mathrm{mm}$ fits the predictions of numerical analysis of the helical MRI in liquid metal experiments [23].
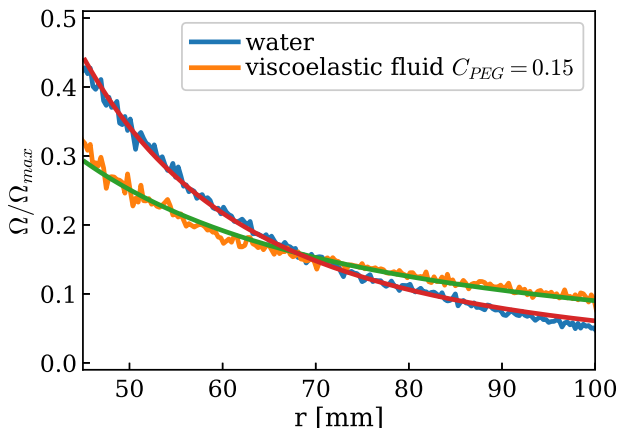
FIG. 6. Profile flattening region observed for a viscoelastic polymer solution (experimental data are shown in orange, the fit is in green) compared to water (experimental data are shown in blue, the fit is in red).

Figure 6 shows the obtained relative rotation profiles Ω/Ω_{max} for viscoelastic and purely hydrodynamic fluid rotation in the region of profile flattening. In the viscoelastic case, a fit of the angular velocity profile yields $\Omega(r) \propto r^{-1.56}$, which is very close to the ideal Keplerian profile of $\Omega(r) \propto r^{-3/2}$. Even though one might think that the flattening of the angular frequency profile can be attributed to the increased internal fluid friction (viscosity), the flow shear profile cannot be affected by the viscosity [21]. The ideal Taylor-Couette profile is modified by only advection of momentum due to a mean radial velocity, the Reynolds stress, or the Maxwell stress or its viscoelastic equivalent [24]. The boundary condition at the pulled-up drain does not allow for mean radial velocity. Figure 4 shows that centrifugal instabilities, which are not possible for the profile in the flattening region, and the angular momentum transport due to the Reynolds stress are balanced by the bottom drag at a far steeper profile. The additional transport causing the profile to flatten can likely be attributed to an enhanced contribution of the viscoelastic Maxwell stress analog.

The evolution of the specific angular momentum profile $l(r) = \Omega r^2$ over several minutes is shown in Fig. 7. Due to the mentioned rod climbing effect, the data acquisition is started only a sufficient time after the drain rotation when this process has reached equilibrium, so it does not influence the rotation profile.
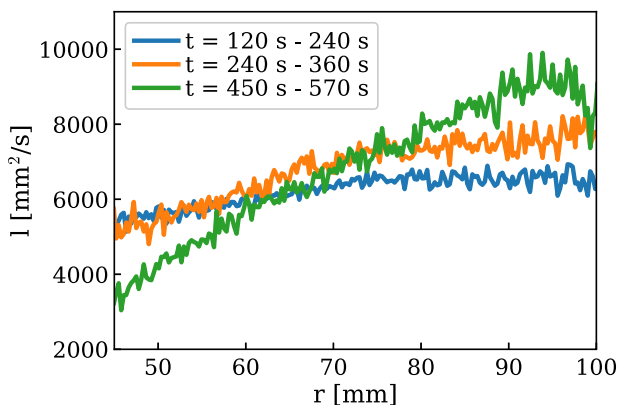

FIG. 7. The specific angular momentum l profile. For $r \gtrsim 100$ mm the specific angular momentum drops, presumably due to the increased influence of ground friction.

Figure 7 shows a transient event that lasts several minutes. Transient growth can occur due to the non-normality of the dynamical evolution operator. The MRI can be subject to nonmodal growth [25]. Due to the analogy of MHD to viscoelastic fluids, non-normal growth should be possible in the viscoelastic fluid as well. During this event, specific angular momentum is reduced for radii smaller than 60 mm and increased for radii larger than 60 mm. The specific angular momentum is transported radially outwards. It should be noted that all profiles shown in Fig. 7 fulfill the Rayleigh stability criterion $dl/dr > 0$. The observed momentum transport can therefore not be explained by Rayleigh's centrifugal instability. The significantly larger viscosity of the viscoelastic solution compared to water ($\nu_{\text{solution}} \sim 10^2 \, \nu_{\text{water}}$) results in a viscous diffusion time similar to the observed time of the transient event in Fig. 7. However, the increased specific angular momentum at the outer radii ($r > 70$ mm) does not seem to be explainable with viscous diffusion. Viscous angular momentum diffusion is driven by a torque $M(r) = \iint r^2 t_{r\theta} d\theta dz$ arising from the viscous stress tensor component $t_{r\theta} \propto r \partial_r \Omega$. For $M(r) = \text{const}$, no net transport of angular momentum occurs. Neglecting the bottom drag, the viscosity damps the profile towards $\Omega(r) \to \Omega_0 r^{-2}$, corresponding to $l(r) = \text{const}$. At $t < 240$ s, $l(r)$ is closest to constant; the observed steepening of $l(r)$ at later times is not expected to be a result of enhanced viscosity. With increasing viscosity, also the bottom drag increases significantly. This is shown in Fig. 5; in the viscoelastic case $\Omega \to 0$ is found at large radii ($r > 100$ mm), whereas in water Ω remains finite. An increase of l, and hence Ω, also cannot be explained by enhanced bottom drag. Therefore, the observed profile steepening cannot be explained by viscous momentum diffusion. This leaves the viscoelastic Maxwell stress as the most apparent cause of the observed transport during this transient event.

V. SUMMARY AND CONCLUSIONS

In summary, whether the shallow water approximation based accretion disklike geometry proposed by Foglizzo *et al.* [11] is suitable to study the dynamics of accretion disks in laboratory experiments was investigated. The setup geometry is closer to the accretion disk geometry than in Taylor-Couette experiments regarding the aspect ratio of radial and coaxial extension. When operating with liquid metals, the shallow water approximation may allow us to investigate a rather large surface area at small fluid volume. Due to cost reasons, the presented experiment prototype was performed with a viscoelastic fluid instead of a liquid metal. Angular momentum transport is the main interest in the dynamics of accretion disks. In the present work, the rotation profiles were measured by means of particle tracking velocimetry. The experiments were performed in water (the purely hydrodynamic case) and in a solution of polyethylene glycol and polyethylene oxide (viscoelastic fluid). The comparison of these measurements allowed us to investigate the importance of MHD effects on angular momentum transport. The experiments performed in the viscoelastic fluid showed a close to Keplerian rotation profile relevant for accretion disk dynamics.

The rotation measurements presented here support the idea of magnetohydrodynamical mechanisms being the likely cause of enhanced outwards transport of angular momentum in accretion disks. They indirectly also support the magnetorotational instability. While the rotation profiles of water appeared to be stable over time, the specific angular momentum decreased at small radii and increased at large radii in a viscoelastic fluid. This result can be seen as enhanced angular momentum transport from small to large radii. An unambiguous identification of the driving instability in the present experiment was not possible. However, the presented prototype experiment showed a first promising result (i.e., outwards angular momentum transport), hopefully motivating more detailed studies in this geometry in the future.

For accretion disks it is expected that both Reynolds and Maxwell stresses lead to outwards transport of angular momentum [13]. In future work, the different contributions of the Reynolds stress and the viscoelastic analog of the Maxwell stress should be estimated. Direct measurements of radial and azimuthal velocities, for example, with laser Doppler velocimetry would allow for measurements of the Reynolds stress. Hereby, the refractive index transition at the open fluid surface is used to determine the surface flow velocities in the radial and azimuthal directions from

the Doppler shift in the reflected light. Measurement of radial fluid flows would also allow us to investigate the impact of Ekman circulation effects. Additional measurements of the axial dynamics would be beneficial. Due to the large contact area at the bottom of the pool, Ekman effects are presumably highly influential in the presented setup geometry [26]. However, whether these effects have a significantly higher impact in a viscoelastic fluid compared to water is not apparent and requires further investigation.

[1] S. A. Balbus and J. F. Hawley, Instability, turbulence, and enhanced transport in accretion disks, Rev. Mod. Phys. **70**, 1 (1998).

[2] S. A. Balbus, Enhanced angular momentum transport in accretion disks, Annu. Rev. Astron. Astrophys. **41**, 555 (2003).

[3] R. Hollerbach and G. Rüdiger, New Type of Magnetorotational Instability in Cylindrical Taylor-Couette Flow, Phys. Rev. Lett. **95**, 124501 (2005).

[4] F. Stefani, T. Gundrum, G. Gerbeth, G. Rüdiger, M. Schultz, J. Szklarski, and R. Hollerbach, Experimental Evidence for Magnetorotational Instability in a Taylor-Couette Flow under the Influence of a Helical Magnetic Field, Phys. Rev. Lett. **97**, 184502 (2006).

[5] M. Seilmayer, V. Galindo, G. Gerbeth, T. Gundrum, F. Stefani, M. Gellert, G. Rüdiger, M. Schultz, and R. Hollerbach, Experimental Evidence for Nonaxisymmetric Magnetorotational Instability in a Rotating Liquid Metal Exposed to an Azimuthal Magnetic Field, Phys. Rev. Lett. **113**, 024505 (2014).

[6] D. R. Sisan, N. Mujica, W. A. Tillotson, Y.-M. Huang, W. Dorland, A. B. Hassam, T. M. Antonsen, and D. P. Lathrop, Experimental Observation and Characterization of the Magnetorotational Instability, Phys. Rev. Lett. **93**, 114502 (2004).

[7] C. Collins, N. Katz, J. Wallace, J. Jara-Almonte, I. Reese, E. Zweibel, and C. B. Forest, Stirring Unmagnetized Plasma, Phys. Rev. Lett. **108**, 115001 (2012).

[8] K. Flanagan, M. Clark, C. Collins, C. M. Cooper, I. V. Khalzov, J. Wallace, and C. B. Forest, Prospects for observing the magnetorotational instability in the plasma Couette experiment, J. Plasma Phys. **81**, 345810401 (2015).

[9] R. Hollerbach, Non-axisymmetric instabilities in magnetic spherical Couette flow, Proc. R. Soc. A **465**, 2003 (2009).

[10] C. Gissinger, H. Ji, and J. Goodman, Instabilities in magnetized spherical Couette flow, Phys. Rev. E **84**, 026308 (2011).

[11] T. Foglizzo, F. Masset, J. Guilet, and G. Durand, Shallow Water Analogue of the Standing Accretion Shock Instability: Experimental Demonstration and a Two-Dimensional Model, Phys. Rev. Lett. **108**, 051103 (2012).

[12] S. Sebold, F. Günzkofer, R. Arredondo, T. Höschen, U. von Toussaint, U. Stroth, and P. Manz, Advective-acoustic cycle in a shallow water standing accretion shock experiment, Phys. Rev. E **102**, 063103 (2020).

[13] M. E. Pessah, C. Chan, and D. Psaltis, The signature of the magnetorotational instability in the Reynolds and Maxwell stress tensors in accretion discs, Mon. Not. R. Astron. Soc. **372**, 183 (2006).

[14] G. I. Ogilvie and M. R. E. Proctor, On the relation between viscoelastic and magnetohydrodynamic flows and their instabilities, J. Fluid Mech. **476**, 389 (2003).

[15] G. I. Ogilvie and A. T. Potter, Magnetorotational-Type Instability in Couette-Taylor Flow of a Viscoelastic Polymer Liquid, Phys. Rev. Lett. **100**, 074503 (2008).

[16] Y. Bai, O. Crumeyrolle, and I. Mutabazi, Viscoelastic Taylor-Couette instability as analog of the magnetorotational instability, Phys. Rev. E **92**, 031001(R) (2015).

[17] S. Boldyrev, D. Huynh, and V. Pariev, Analog of astrophysical magnetorotational instability in a Couette-Taylor flow of polymer fluids, Phys. Rev. E **80**, 066310 (2009).

[18] J. C. Crocker and D. G. Grier, Methods of digital video microscopy for colloidal studies, J. Colloid Interface Sci. **179**, 298 (1996).

[19] S. Fromang and G. Lesur, Angular momentum transport in accretion disks: A hydrodynamical perspective, EAS Publ. Ser. **82**, 391 (2019).

[20] H. Ji, M. Burin, E. Schartman, and J. Goodman, Hydrodynamic turbulence cannot transport angular momentum effectively in astrophysical disks, Nature (London) **444**, 343 (2006).

[21] Y. Bai, Study of viscoelastic instability in Taylor-Couette system as an analog of the magnetorotational instability, Ph.D. thesis, Universite du Havre, 2015, available online at https://tel.archives-ouvertes.fr/tel-01255319.

[22] K. Weissenberg, A continuum theory of rheological phenomena, Nature (London) **159**, 310 (1947).

[23] G. Mamatsashvili, F. Stefani, A. Guseva, and M. Avila, Quasi-two-dimensional nonlinear evolution of helical magnetorotational instability in a magnetized Taylor–Couette flow, New J. Phys. **20**, 013012 (2018).

[24] E. Schartman, H. Ji, M. Burin, and J. Goodman, Stability of quasi-Keplerian shear flow in a laboratory experiment, Astron. Astrophys. **543**, A94 (2012).

[25] J. Squire and A. Bhattacharjee, Nonmodal Growth of the Magnetorotational Instability, Phys. Rev. Lett. **113**, 025006 (2014).

[26] M. J. Burin, H. Ji, E. Schartman, R. Cutler, P. Heitzenroeder, W. Liu, L. Morris, and S. Raftopolous, Reduction of Ekman circulation within Taylor-Couette flow, Exp. Fluids **40**, 962 (2006).